

# Disk motion – a new control element in high-brightness solid state laser design

**Santanu Basu**

*Sparkle Optics Corporation*

655 Deep Valley Drive, Suite 170 Rolling Hills Estates, CA 90274 USA

Tel (310) 265-8601

[basu@sparkleoptics.com](mailto:basu@sparkleoptics.com)

<http://www.sparkleoptics.com>

**Arun Sridharan**

*Consultant to Sparkle Optics Corporation*

*Ginzton Laboratory, Stanford University, Stanford, CA 94305 USA*

**Abstract:** The brightness of cw and quasi cw solid state lasers of conventional designs is limited by stress fracture and uncorrectable phase aberration in thermally loaded stationary gain medium. By introducing physical motion of the gain medium as a new control element in the design of solid state lasers, we show the potential to significantly increase the brightness of cw and quasi cw solid state lasers. In this paper, we develop the design equations of rotary disk lasers and illustrate the design of a 1-kilowatt single mode Yb-YAG rotary disk laser.

© 2004 Optical Society of America

**OCIS codes:** (140.0140) Lasers and laser optics; (140.3580) Lasers, solid-state; (140.5680) Rare earth and transition metal solid-state lasers; (140.6810) Thermal effects

---

## References

1. M. Wickham, J. Anderegg, S. Brosnan, D. Hammons, H. Komine and M. Weber, "Coherently Coupled High Power Fiber Arrays," paper MA4, presented at the Advanced Solid State Photonics Conf., Santa Fe, NM, 2004.
2. C.H. Liu, A. Galvanauskas, B. Ehlers, F. Doerfel, S. Heinemann, A. Carter, K. Tankala and J. Farroni, "810-W single transverse mode Yb-doped fiber laser," paper PD2-1, presented at the Advanced Solid State Photonics Conf., Santa Fe, NM, 2004.
3. F. Butze, M. Larionov, K. Schuhmann, C. Stolzenburg and A. Giesen, "Nanosecond pulsed thin disk Yb:YAG lasers," paper WA4, presented at the Advanced Solid State Photonics Conf., Santa Fe, NM, 2004.
4. G. Holleman, G. Harpole, H. Injeyan, R. Moyer, M. Valley, J. Machan, R. St. Pierre, J. Berg and L. Marabella, "Modelling High Brightness kW Solid State Lasers," Proc. SPIE **2989**, 15-22 (1997).
5. M. Rotter, C. Brent Dane, S. Gonzales, R. Merrill, S. Mitchell, C. Parks and R. Yamamoto, "The solid-state heat-capacity laser," paper PD8-1, presented at the Advanced Solid State Photonics Conf., Santa Fe, NM, 2004.
6. S. Basu and R.L. Byer, "Fiber coupled diode pumped moving solid state laser," U.S. Patent 4,890,289, 1990.
7. S. Basu, *A high peak and high average power Nd:glass moving slab laser for soft X-ray generation*, (Stanford University PhD dissertation, Stanford, CA 1988), pp. 180-188.
8. S. Basu and R.L. Byer, "Diode-pumped moving-disc laser: a new configuration for high average power generation," Opt. Quantum Electron., **23**, 33-37 (1990).
9. S. Basu, J. Depsky, R.S. Shah and T. Endo, "Numerical Designs of 100-kW Average Power Solid State Lasers," in *Modeling and simulation of higher-power laser systems IV*, U. Farrukh and S. Basu, eds., Proc. SPIE **2989**, 2-14 (1997).

10. A. H. Paxton, S.M. Massey, J.B. McKay and H.C. Miller, "Rotating-Disk Solid-State Lasers, Thermal Properties," in *Laser Resonators and Beam Control VII*, A. Kudryashov, ed., Proc. SPIE **5333**, 12-17 (2004).
11. S. Basu and R.L. Byer, "40-W average power, 30-Hz moving-slab Nd-glass laser," *Opt. Lett.*, **11**, 617-619 (1986).
12. J. Korn, T.H. Jeys and T.Y. Fan, "Continuous wave operation of a diode-pumped rotating Nd-glass disk laser," *Opt. Lett.*, **16(24)**, 1741-1743 (1991).
13. S. M. Massey, J.B. McKay, T.H. Russell, A.H. Paxton, S. Basu, and H.C. Miller, "Diode Pumped Nd:YAG and Nd:Glass Spinning Disk Lasers", submitted for publication in *JOSA B* (2004).
14. S. Basu and H.C. Miller, "A 40-W single mode Yb-YAG rotary disk laser", in *Solid state and diode laser technology review*, S. Ross, ed., (Directed Energy Professional Society, 2004), p. P-43.
15. T.Y. Fan and R.L. Byer, "Modeling and cw operation of a quasi-three-level 946 nm Nd:YAG laser," *IEEE J. Quantum Electron*, **QE-23**, 605-612 (1987).
16. W.P. Risk, "Modeling of longitudinally pumped solid-state lasers exhibiting reabsorption losses," *J. Opt. Soc. Am B*, **5**, 1412-1423 (1988).
17. P. Peterson, A. Gavrielides and P. Sharma, "Cw theory of a laser diode pumped two-manifold solid state laser," *Opt. Commun.*, **109**, 282-287 (1994).
18. C. D. Nabors, J. Ochoa, T. Y. Fan, A. Sanchez, H. K. Choi, and G. W. Turner, "Ho:YAG Laser Pumped by 1.9- $\mu\text{m}$  Diode Lasers," *IEEE J. Quantum Electron*, **31**, 1603-1605 (1995).
19. W.W. Rigrod, "Saturation effects in high gain lasers," *J. Appl. Phys.*, **36**, 2487-2490 (1965).
20. A.E. Siegman, *Lasers* (University Science Books, 1986).
21. R.B. Bird et al, *Transport Phenomena* (John Wiley & Sons, 1960).
22. J.M. Eggleston, T.J. Kane, K. Kuhn, J. Unternahrer and R.L. Byer, *IEEE J. Quantum Electron.*, "The slab geometry laser. I-Theory," **QE-20**, 289-301 (1984).
23. T.Y. Fan, "Heat generation in Nd:YAG and Yb:YAG," *IEEE J. Quantum Electron*, **29**, 1457-1459 (1993).

## 1. Introduction

The waste heat in any solid state laser medium causes uncorrectable phase aberration in the path of the laser beam due to thermal and stress induced refractive index change. It imposes fundamental limitation on brightness of a conventional cw or quasi cw solid state laser in which the gain medium is stationary. This problem is unavoidable, and is not fully correctable using adaptive optics without significant power loss. The state of the art solid state laser designs for high cw brightness (high cw power at good beam quality) include phase-locked lasers [1], Yb fiber lasers of large mode area [2], thin disk lasers [3], zig-zag slab lasers with active phase correction [4], and intermittently operated heat capacity lasers [5].

To compare different laser sources, we define a laser brightness factor  $B_L$

$$B_L = P / (\lambda BQ)^2 \quad (1)$$

where  $P$  is the laser power,  $\lambda$  is the wavelength, and  $BQ$  is a geometrically averaged laser beam quality ( $=M^2$ ) in two orthogonal directions. The peak intensity,  $I$ , at the focus when the laser beam is focused using an optic of diameter,  $D$ , and focal length,  $f$ , is simply

$$I = B_L \pi(D/f)^2 / 4 \quad (2)$$

The incentive to improve the laser brightness factor stems from those applications which require high cw peak intensity at long ranges. Table 1 shows the magnitude of this factor,  $B_L$ , for several state of the art solid state laser systems [1-5]. It is to be noted that among all laser systems, currently the chemical lasers have the highest cw laser brightness ( $B_L$ ), which is much greater than that of solid state lasers. There is however intense effort to improve the average brightness of solid state lasers.

The objective of this paper is to analytically investigate an "unconventional" design that has the potential of significantly increasing the laser brightness factor  $B_L$  in solid state lasers. The "unconventional" design is the rotary disk laser design, which was invented at Stanford in

1987 by Basu and Byer [6]. The architecture of using fiber-coupled diodes to pump arrays of rotary disk lasers and moving slab lasers to generate hundreds of kilowatt of average power was first conceptualized by Basu in 1987 [7]. Rotary disk lasers utilize the “motion” of the solid state laser medium as an independent control variable to overcome the thermal limitations in brightness scaling.

Table 1. Performance of state of the art high brightness solid state lasers

Laser Type	Reference	Average Power, P (W)	Wavelength, $\lambda$ ( $\mu\text{m}$ )	BQ ( $\sim\text{M}^2$ )	Laser Brightness Factor, $B_L$ ( $\text{W}/\mu\text{m}^2$ )
Phase-locked Yb fiber	1	155	1.05	1.32	81
Large Mode Area Nd/Yb fiber	2	810	1.092	1.42	337
Thin disk Yb-YAG	3	101.4	1.03	1.14	74
Nd-YAG slab, phase conjugated	4	900	1.06	1.5	356
Heat capacity laser	5	10,000 (for 4 s burst)	1.05	(65% of Power in a spot with BQ=3)	655

The laser performance analysis of rotary disk lasers for 4-level laser systems was reported by Basu and Byer [8] and thermal analyses of rotary disk lasers were carried out by Basu et al [9], and Paxton *et al.* [10]. The first experimental demonstration of a 40-W solid state laser in which the gain medium was not stationary was done by Basu and Byer in 1986 [11]. The first experimental result on a diode-pumped rotary disk laser was reported by Fan *et al.* in 1990 [12]. After 13 years of no activity in this field, rotary disk laser operation in Nd-YAG and Nd-glass was conducted by Massey et al in 2003 [13]. Very recently, Basu and Miller reported the operation of a 53-W single-mode fiber-coupled rotary disk laser in Yb-YAG [14].

There is renewed interest in rotary disk laser architecture [13-14] for power and brightness scaling in solid state lasers. In this paper, we develop for the first time the design equations of a rotary disk laser in either a 3-level or a 4-level solid state laser system that can be helpful in this brightness scaling effort. A typical design of a 1-kW single-mode rotary disk Yb-YAG laser is illustrated.

## 2. Rotary disk laser

A schematic of the rotary disk laser is shown in Fig. 1. The laser medium in the form of a thin disk is rotated in between two cooling plates, which act as heat sinks. The pump beam is focused to a small spot on the face of the disk away from the center. The rotation of the disk continuously removes the heated material from the pumped area and brings in cold material to be pumped in a regenerative fashion. Heat is removed from the disk by conduction across the gas gap between the laser medium and the heat sink. While the laser is operating in one part of the disk near the pumped region, the heat is being dissipated over a much larger annular area away from the laser extraction region. The pumping and the laser extraction regions are thus physically separated from the heat transfer region. While rotation is the simplest form of motion, a “rotary disk laser” may also employ combination of translation, rotation, vibration or even intermittent mode of laser operation depending on the application. The simple concept of non-stationary gain medium as is described here has met with severe resistance in the past, since the gain media in nearly all solid state lasers to date have remained stationary.

The pump beam and the laser beam can be oriented with respect to each other in almost an unlimited number of ways. When the pump and the resonator beams propagate almost along the same direction in the laser medium, the rotating disk laser may be considered “face-

pumped”, or “end-pumped”. When the laser beam and the resonator beam are nearly normal to each other, the rotating disk laser may be considered “side pumped”. There are advantages and disadvantages of each of these orientations depending on the application.

There is also another remarkable feature of a rotary disk laser. Unlike any other solid state lasers of today, the laser beam in the resonator may not even need to overlap with the pump beam in the medium. This is because the disk motion also transports excited atoms away from the pumped region, and the excited atoms may be brought into the resonator for laser power extraction. A single disk may be used to multiplex a number of pump sources, and at the same time, to operate a number of lasers or amplifiers which are physically separated but which extract laser energy from the same rotary disk.

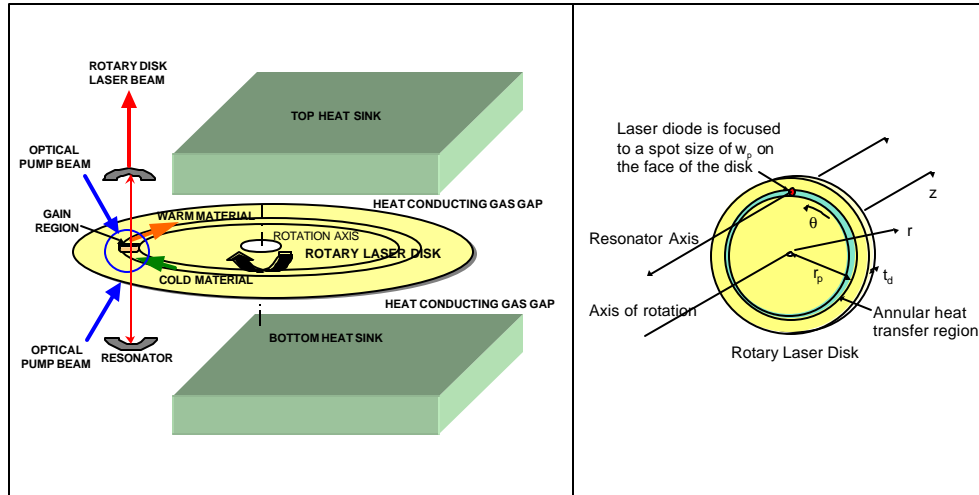


Fig. 1. Schematic of a typical rotary disk laser, and, the coordinate system used in the analysis

The traditional design elements which control the performance of high-brightness solid state lasers are the properties of the gain medium, the shape of the medium, the optical pump source, the mode of pumping and laser power extraction. Some other design considerations are phase locking of independent lasers, intermittent laser operation, and use of beam correction technologies. The “motion of the gain medium” can be thought of a new control element useful in future designs of high-power and high-brightness solid state lasers.

The motion of the laser disk through the resonator section and the heat transfer region isolates laser action from heat dissipation. It significantly reduces the temperature rise and thermal stresses in the gain region. This in turn significantly reduces thermally induced uncorrectable phase aberration within the resonator. This should result in a considerable increase in single mode power extraction from a rotary disk laser. The rotary disk lasers have a potential for significantly increasing the brightness of solid state lasers beyond the current state of the art. “Rotary Disk Laser” is a pending trademark of Sparkle Optics.

### 3. Rotary disk laser analysis for Yb-YAG

#### 3.1 Laser analysis

The cw operation is analyzed in this section. The energy level diagram of Yb -YAG is shown in Fig. 2.

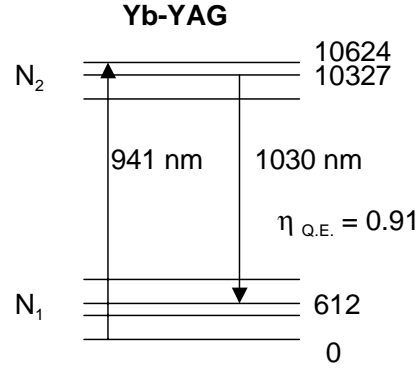


Fig. 2. Energy level diagram of Yb-YAG

We apply the analysis of quasi-three-level end-pumped laser systems [15-18] to formulate the design of Yb-YAG rotary disk lasers. The relevant expressions for population difference for pump absorption (between  $0 \text{ cm}^{-1}$  and  $10624 \text{ cm}^{-1}$ ),  $\Delta N^{\text{pump}}$ , and for laser emission (between  $10327 \text{ cm}^{-1}$  and  $612 \text{ cm}^{-1}$ ),  $\Delta N^{\text{laser}}$ , taking Boltzmann factors,  $f$ , are given by

$$\Delta N^{\text{pump}} = f_1^{\text{pump}} N_1 - f_2^{\text{pump}} N_2 \quad (3)$$

$$\Delta N^{\text{laser}} = f_2^{\text{laser}} N_2 - f_1^{\text{laser}} N_1 \quad (4)$$

where the superscripts pump and laser denote pump and laser, and subscripts 1 and 2 denote lower and upper manifolds respectively. The Boltzmann factors depend on temperature, the energy levels associated with absorption and emission, and the splitting of upper and lower manifolds. The threshold condition determines the length-integrated inverted population density,  $\Delta N^{\text{laser l}} = \int_{\text{gain medium}} \Delta N^{\text{laser}} dx$ , which is given by

$$\Delta N^{\text{laser l}} = (1 / (2 \sigma^{\text{laser}})) (-\ln((1 - L_c)R)) \quad (5)$$

The length-integrated upper manifold population,  $N_2^{\text{l}}$ , and the length-integrated population difference for pump absorption,  $\Delta N^{\text{pump l}}$ , are obtained keeping track of the distribution of the total population in two manifolds.

$$N_2^{\text{l}} = (1 / (f_1^{\text{laser}} + f_2^{\text{laser}})) (\Delta N^{\text{laser l}} + f_1^{\text{laser}} N_0 L^{\text{pump}}) \quad (6)$$

where  $N_0$  is the ion density, and  $L^{\text{pump}}$  is the beam path through the pumped region.

$$\Delta N^{\text{pump l}} = f_1^{\text{laser}} N_0 L^{\text{pump}} - (f_1^{\text{pump}} + f_2^{\text{pump}}) N_2^{\text{l}} = f_1^{\text{laser}} N_0 L^{\text{pump}} - ((f_1^{\text{pump}} + f_2^{\text{pump}}) / (f_1^{\text{laser}} + f_2^{\text{laser}})) (\Delta N^{\text{laser l}} + f_1^{\text{laser}} N_0 L^{\text{pump}}) \quad (7)$$

The efficiency for the conversion of the pump light into the laser output depends on several efficiency factors which are  $\eta_{\text{abs}}$ , the absorption efficiency of the incident pump light,  $\eta_{\text{c}}$ , the efficiency of coupling the pump light into the laser medium,  $\eta_{\text{overlap}}$ , the efficiency of coupling into the recirculating lasing mode volume in the cavity (which is dependent on diffraction effects),  $\eta_{\text{quantum}}$  which is the quantum efficiency, and  $\eta_{\text{ext}}$ , the external output coupling efficiency.

The absorption efficiency in a face-pumped quasi-three level laser can be shown to be

$$\eta_{\text{abs}}^{\text{pump}} = (1 - \exp(-\sigma^{\text{pump}} \Delta N^{\text{pump l}})) (1 + R^{\text{pump}} \exp(-\sigma^{\text{pump}} \Delta N^{\text{pump l}})) \quad (8)$$

$R^{\text{pump}}$  is the efficiency of reflecting the unused pump radiation into the gain region. The quantum efficiency is given by

$$\eta_{\text{quantum}} = \lambda_{\text{pump}} / \lambda_{\text{laser}} \quad (9)$$

where  $\lambda_{\text{pump}}$  is the weighted average of pump wavelength and  $\lambda_{\text{laser}}$  is the laser wavelength. Rigrod formula [19] is used to describe the external coupling efficiency, in which  $R$  is the output mirror reflectivity, and  $L_c$  is the total round trip loss in the cavity.

$$\eta_{\text{ext}} = (1-R) / ((1-R) + L_c \sqrt{R/(1-L_c)}) \quad (10)$$

We assume that the pump beam is focused on the face of the disk to a gaussian spot size of  $w_p$  at a radius  $r_p$  from the disk center as shown in figure 1. The threshold pump power,  $P_{\text{th}}$ , and the slope efficiency,  $\eta_{\text{slope}}$  for cw pumping and extraction for the 3-level laser system are obtained using analysis similar to the analysis of end-pumped 4-level laser systems [20].

$$P_{\text{th}} = (h\nu^{\text{pump}} N_2^l (\pi w_p^2/2) / \tau) / (\eta_{\text{abs}} \eta_c \eta_{\text{overlap}}) \quad (11)$$

$$\eta_{\text{slope}} = \eta_{\text{abs}} \eta_{\text{ext}} \eta_c \eta_{\text{overlap}} \eta_{\text{quantum}} \quad (12)$$

and finally, the laser output power is given by

$$P_{\text{out}} = \eta_{\text{slope}} (P_{\text{in}} - P_{\text{th}}) \quad (13)$$

As a check, the analysis given above can also be applied to 4-level laser systems by making the substitutions  $f_1^{\text{pump}} = 1$ ;  $f_1^{\text{laser}} = 0$ ; and  $f_2^{\text{pump}} = 0$ , which give

$$\Delta N^{\text{pump}} = f_1^{\text{pump}} N_1 - f_2^{\text{pump}} N_2 = N_1 \quad (14)$$

$$\Delta N^{\text{laser}} = f_2^{\text{laser}} N_2 - f_1^{\text{laser}} N_1 = f_2^{\text{laser}} N_2 \quad (15)$$

For some 4-level materials such as Nd-glass, in which the lower laser level is close to the ground state, the fractional population in the lower laser level  $f_1^{\text{laser}}$  may not be zero at the operating temperature. In these cases, Eq. (4) is more appropriate than Eq. (15).

This concludes the laser performance analysis of the rotary disk laser.

### 3.2 Thermal analysis of rotary disk laser

Thermal analyses of rotary disk lasers have been previously reported in references 8-10. In this section, we present for the first time the engineering analysis of rotary disk lasers that is the basis of the 1-kW single-mode rotary disk laser design in section 4. A more detailed analysis of the thermal and stress distribution in a rotary disk laser is being investigated by the authors which will be documented in the future.

The coordinate system used in the analysis is shown in Fig. 1. The heat equation in cylindrical coordinate system  $(r, \theta, z)$  [21] as applied to the rotary laser disk is

$$C_p (\partial T / \partial t + (V_\theta / r) \partial T / \partial \theta) = k (1/r \partial / \partial r (r \partial T / \partial r) + (1/r^2) \partial^2 T / \partial \theta^2 + \partial^2 T / \partial z^2) + Q \quad (16)$$

where  $C_p$  is the specific heat per unit volume,  $V_\theta$  is the linear velocity in the azimuthal direction,  $T$  is the temperature,  $k$  is the thermal conductivity, and  $Q$  is the heat absorption rate per unit volume. The plane  $z=0$  is half way between the two circular faces of the rotary disk.

Equation (16) applies in all layers in the path of conductive heat flow. In the disk ( $z=0$  to  $t_d/2$ ),

$$k = k_d, \rho = \rho_d, C_p = C_{p,d} \text{ and } Q = \text{heat dissipation from pumping} \quad (17)$$

where  $t_d$  is the disk thickness. In the gap ( $z = t_d/2$  to  $t_g + t_d/2$ ),

$$k = k_g, \rho = \rho_g, C_p = C_{p,g} \text{ and } Q = 0 \quad (18)$$

In the heat sink ( $z > t_g + t_d/2$ ),

$$k = k_{\text{HS}}, \rho = \rho_{\text{HS}}, C_p = C_{p,\text{HS}} \text{ and } Q = 0 \quad (19)$$

Heat is being deposited within the pumped volume, which is stationary in the coordinate system, which is fixed with the resonator and the optical pump source. The heat is removed from the disk to the heat sinks over an annular region that is also stationary in the same coordinate system as above. After the rotary disk laser is turned on, the temperature rises in the annular section of the disk until a steady state condition develops. In this steady state condition, and in the coordinate system fixed with the resonator, there is a fixed temperature profile in the space occupied by the disk.

There is temperature increase from the cold end of the pumped region to the hot end in the azimuthal direction of disk rotation, followed by a gradual temperature decrease from the hot end to the cold end along the same azimuthal direction. A nearly linear azimuthal thermal

gradient is superimposed on the nearly quadratic temperature profile in the z-direction within the disk. This azimuthal temperature gradient should cause a small angular displacement of the beam, which is easily corrected by tilting the resonator optics. The thermal gradient in the r direction can be made to be orders of magnitude smaller than in the z direction, by forcing the heat flow to be in the z direction only. The thermal lensing due to temperature profile in the r-direction has been experimentally shown to be very small in YAG [13-14].

In the steady state case, assuming  $\partial T/\partial r$ , and,  $\partial T/r\partial\theta \ll \partial T/\partial z$ , Eq. (16) simplifies to

$$k \partial^2 T/\partial z^2 + Q = 0 \quad (20)$$

The heat conduction equation within the gain medium is identical to that of a face cooled slab in a slab laser [22]. In essence, the pumped band on the rotary disk may be uncoiled to a slab of width  $2w_p$  and thickness  $t_d$ . The dissipated heat in the equivalent slab is transferred to a cold plate through a thin layer of gas of thickness,  $t_g$ , and thermal conductivity,  $k_g$ ,

Assuming symmetric pumping and cooling on two faces, the boundary conditions are

$$\partial T/\partial z = 0 \text{ at } z=0; \text{ and, } -k_d \partial T/\partial z \text{ in disk} = -k_g \partial T/\partial z \text{ in gas at } z= t_d/2 \quad (21)$$

We assume a perfect heat sink and assume that the temperature at the heat sink surface in contact with the gas is constant. This is written as  $T = T_{HS}$  at  $z = t_g + t_d/2$ . This is a good approximation in most cases, in which the heat sink is made of a high-conductive material, and the heat sink is aggressively cooled with internal fluid flow.

The dissipated power,  $P_h$  is estimated by

$$P_h = F_{eh} (1 - \lambda_{pump}/\lambda_{laser}) \eta_{abs} P_{in} \quad (22)$$

The factor  $F_{eh}$  takes into account excess heat generated in the gain medium due to non radiative relaxations [23]. We have assumed a conservative value of 1.5 for  $F_{eh}$  in Section 4 of this paper.

The time averaged pumped volume is given by

$$V_p = 4 \pi w_p r_p t_d \quad (23)$$

The time averaged heat dissipation per unit volume is given by

$$Q = P_h / V_p \quad (24)$$

We assume that the heat deposition is uniform within the pumped volume, and the heat flow is primarily in the z direction. In order to estimate the maximum stress in the disk, we confine our attention to the quadratic temperature profile in the z direction. The effect of the nearly linear azimuthal temperature distribution on the stress in the disk is assumed to be small. The quadratic temperature profile in the annular region of the disk is obtained from Eqs. (20)-(21)

$$T = T_{HS} + (P_h/V_p) t_g t_d / (2k_g) + ((P_h/V_p) / 8 k_d) (t_d^2 - 4z^2) \quad (25)$$

The maximum temperature is at  $z=0$ , and is given by

$$T_{max} = T_{HS} + (P_h/V_p) t_g t_d / (2k_g) + (P_h/V_p) t_d^2 / 8 k_d \quad (26)$$

The maximum temperature difference between the disk surface ( $z= t_d/2$ ) and the disk midplane ( $z=0$ ) within the pumped region is given by

$$T_{diff, max} = (P_h/V_p) t_d^2 / 8 k_d \quad (27)$$

The maximum stress in the disk is tensile. It is on the disk surface, and is related to the maximum temperature difference,  $T_{diff, max}$ . The maximum stress,  $\sigma_{max}$ , is given by

$$\sigma_{max} = (P_h/V_p) t_d^2 / 12 M_s \quad (28)$$

Where  $M_s$  is a material stress figure of merit, defined as  $M_s = (1-\nu) k_d / \alpha E$ , in which  $\nu$  is the Poisson ratio,  $\alpha$  is the thermal expansion coefficient, and  $E$  is the Young's modulus.

The required disk rotation rate is determined primarily by two factors: allowable temperature rise in the material as it traverses the pumped region which sets a lower limit; and azimuthal transport of the excited atoms, followed by spontaneous emission loss. A

simplified analysis, which yields a fairly accurate and quick estimate of the required rotation speed, is given here.

The residence time of the lasing atoms through the pumped region in one revolution of the disk is given by

$$t_{\text{pump}} = 2 w_p / (2\pi r_p v_{\text{rot}}) \quad (29)$$

where,  $v_{\text{rot}}$  is the disk rotation rate in Hz. Assuming adiabatic condition, the temperature rise,  $\Delta T_{\text{pumped region}}$ , in the material as it passes through the pumped region is

$$\Delta T_{\text{pumped region}} = P_h / (\pi^2 w_p t_d r_p C_p v_{\text{rot}}) \quad (30)$$

The minimum disk rotation rate,  $v_{\text{rot, min}}$  is set by the maximum allowable temperature difference,  $\Delta T_{\text{pumped region, max}}$  across the pumped region, and is calculated using Eq. (30).

The decay of the population inversion in absence of laser extraction is given by

$$f_{\text{decay}} = \exp(-t / \tau_{\text{lifetime}}) \quad (31)$$

The rotation of the disk drags a fraction of the inverted population along the  $\theta$  direction. This new feature of the rotating disk laser may be exploited to design lasers where the pumped region, the laser extraction region and the heat transfer region are physically isolated.

The width of the gain region,  $2w_{p,\text{rot}}$  in the  $\theta$  direction in presence of disk rotation has been approximated to be

$$2w_{p,\text{rot}} = 2 w_p + 2\pi r_p v_{\text{rot}} \tau_{\text{lifetime}} \quad (32)$$

For a maximum of factor of 2 increase in the width of the gain region, the rotation speed should be less than

$$v_{\text{rot, max}} = w_p / (\pi r_p \tau_{\text{lifetime}}) \quad (33)$$

### 3.3 Performance Enhancement Factor, $S$

The thermal performance of the rotary disk laser is expected to be better than the traditional solid state lasers in which the gain medium is stationary. The available heat transfer area in a rotary disk laser can be approximated as

$$A_h (\text{rotary}) = 8 \pi w_p r_p \quad (34)$$

While the available heat transfer area in a stationary end-pumped disk laser with the same pump spot size,  $w_p$  is

$$A_h (\text{stationary}) = 2 \pi w_p^2 \quad (35)$$

We define a solid state laser performance enhancement factor,  $S$  as

$$S = A_h (\text{rotary}) / A_h (\text{stationary}) = 8 \pi w_p r_p / 2 \pi w_p^2 = 4 r_p / w_p \quad (36)$$

As an example,  $r_p = 20$  mm,  $w_p = 0.9$  mm for the design given in section 4. For this case, the solid state laser performance enhancement factor,  $S = 88$ . It means that a rotary disk laser can be pumped with 88 times more power than a stationary disk laser with the same  $w_p = 0.9$  mm. Comparing these two cases, the rotary disk laser can be designed to produce 88 times more laser power than the stationary disk laser.

As compared to a solid state laser with a stationary gain medium, the lensing and higher order aberrations are smaller simply because the temperature rise in the pumped region is much smaller. The phase aberrations due to temperature and stress induced index change, and risk of thermal stress fracture are significantly reduced. In addition, the beam propagation through the disk averages all temperature and stress gradients which lead to slab-like operation with no biaxial focusing. For Brewster angle operation, the laser beam is polarized. Because the pumped region is away from the disk center, depolarization is significantly reduced as has been confirmed experimentally [13,14].

This concludes the thermal analysis of the rotary disk laser.

## 4. Application of Analysis

### 4.1 Rotary Disk Yb-YAG laser with 1 disk

To illustrate a typical rotary disk laser design, we have chosen a Yb-YAG disk of 4.5 cm diameter and 4 mm thickness ( $t_d$ ), with 5% doping. The disk is rotated at a typical speed of 600 rpm in between two cooling plates, which act as heat sinks. The gap between the Yb-YAG disk and the heat sink is assumed to be 0.1 mm ( $t_g$ ), and is filled with helium. The heat sink surface temperature is assumed to be maintained at 278 K ( $T_{HS}$ ) by internal water flow.

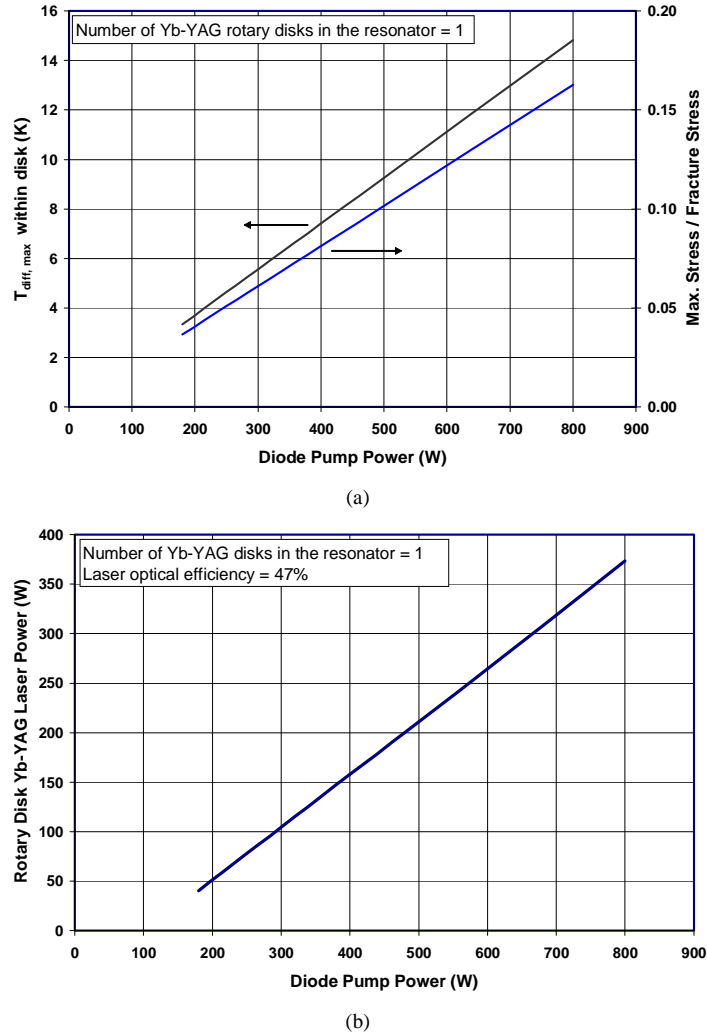


Fig. 3. (a) Calculated maximum temperature difference within the rotary disk Yb-YAG vs. pump power during laser operation; calculated maximum stress divided by fracture stress of Yb-YAG vs. pump power is shown in secondary y axis; (b) Calculated single-mode output power from a Rotary Disk Yb-YAG laser containing one 45-mm diameter laser disk

Typical laser diode for optical pumping is a fiber-coupled diode laser at 941 nm ( $\lambda_{pump}$ ). Each disk is assumed to be pumped with up to 800 W of power ( $P_{in}$ ) using one or two fiber coupled diode lasers. The end of the pump beam delivery fiber is imaged on the disk with focusing optics to a pump spot radius of  $w_p = 0.9$  mm. The Pump spot is assumed to be

located at  $r_p = 2$  cm from the center of the disk. The polarization of the pump laser does not affect the laser performance in Yb-YAG.

Using the analysis presented in the previous section, we have calculated the expected performance of the rotary disk Yb-YAG laser. With a 1 m cavity, a flat output mirror and a 5-m radius of curvature high reflective concave mirror, the laser mode area within the crystal matches the pumped area and the mode overlap factor is 1. This is the design for single-transverse-mode operation.

The thermal performance of the 1-disk rotary disk Yb-YAG laser is shown in Fig. 3(a). The design rotation rate is 11.4 Hz, at which there is a 4 deg K linear temperature difference across the pumped region in the azimuthal direction at 800 W of pump power. The maximum temperature difference,  $T_{\text{diff, max}}$ , which is given by Eq. (27), is plotted in Fig. 3a as a function of pump power. The maximum temperature difference is only 14.8 K at the highest pump power. The maximum stress in the disk also increases with pump power, and remains at 16.3% of fracture stress at the maximum pump power as shown in Fig. 3(a). This is a safe operating region for the Yb-YAG disk laser.

The rotary disk Yb-YAG laser output power is shown in Fig. 3(b). The output coupler is chosen to be 33%. The figure shows that 373 W of laser power can be extracted at 800 W of pump power from a single Yb-YAG laser disk. Because of the designed overlap between the resonator and the pump modes, and the absence of thermally induced focusing, the beam is expected to be single mode. The projected laser optical efficiency is 47% in single mode operation. This design is conservative and is realizable with current technology.

Because the propagation direction is along the temperature gradient, there is no first order focusing in rotary disk laser. The temperature gradient along the azimuthal direction causes a small angular displacement of the beam, which does not degrade beam quality. A small amount of jitter in the output beam is expected because of the disk wobble and fabrication tolerances. However, this jitter is repetitive with a periodicity of 11.4 Hz, which may be compensated using the tilt control hardware of an adaptive optics system.

#### *4.2 Power Scaling with multiple disks*

The thermally induced phase aberration in the laser beam propagating through each rotary disk is controllable using the disk rotation as the control variable. The design given in the previous section should have very little thermally induced phase aberration as discussed. This allows a building block approach to power scaling, which is accomplished by stacking a number of rotary laser disk modules (disk and the pump source) in the same resonator.

For the 1-kW design illustration, we have considered a laser design with three identical rotary disks of the same characteristics as the one used in Fig. 3. Each 45-mm diameter Yb-YAG rotary disk is pumped with 800 W of pump power. The rotary disk laser output power is shown as a function of diode pump power in Fig. 4. A single laser with 3 identical Yb-YAG rotary disk modules is expected to produce 1 kW of cw output power at 2 kW of total diode pump power as shown in Fig. 4. The projected diode laser to Yb-YAG laser optical efficiency is 50%. At 2 kW of total pump power in 3 disks, the round trip gain is calculated to be  $\exp(14.4)$ . The loss due to lower level absorption is much smaller than the round trip gain. At this gain, an unstable resonator is a good option for efficient single-mode power extraction. An unstable resonator of magnification 2 is used in the calculations. The beam quality is expected to be single mode, and defined by the unstable resonator. This design scales to significantly greater than 1 kW using a large number of disks in an oscillator-amplifier configuration, the designs of which will be documented in the future.

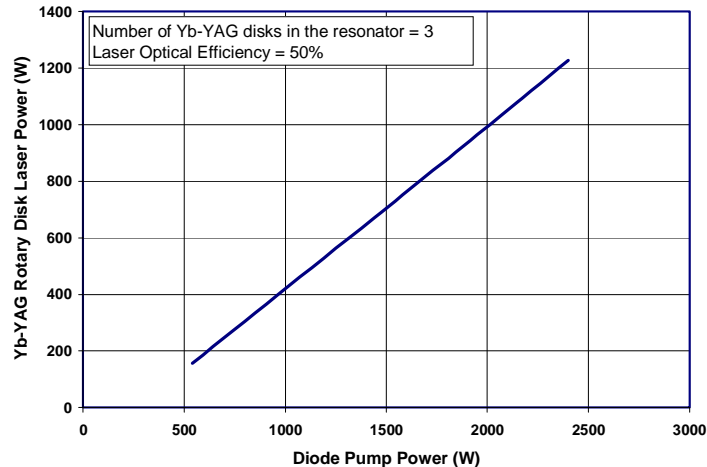


Fig. 4. Calculated single-mode output power from a Yb-YAG rotary disk laser containing 3 identical 45-mm diameter laser disks in an unstable resonator cavity with magnification 2.

## 5. Conclusion

The rotary disk lasers have a unique combination of features, which set it apart from all other solid state lasers. These are:

1. High gain due to small pump focus spot, not limited by thermal effects; it is indeed possible to pump a laser material at the highest pump power density in a rotary disk laser.
2. Low loss due to short path length through the gain medium
3. Significantly reduced mode-clipping loss in a clear aperture amplifier
4. High pulsed energy and high peak power due to scalable beam size
5. Efficient utilization of diode laser pump power and high laser efficiency in face-pumping
6. Efficient thermal management minimizes phase aberration, depolarization and stress in each laser disk, enabling a building block approach for high power lasers
7. Ability to multiplex a number of pump sources, amplifier beams and laser resonators in a single rotary disk
8. High reliability and long lifetime due to conductive cooling through a gaseous medium,
9. Availability of high precision rotational machinery for both ground and space.

The major advantage of rotary disk lasers over fiber lasers is expected to be in the pulsed operation and in the amplifier operation. Because there is no requirement of mode confinement, the laser beam can be expanded in the rotary disk for amplification without mode-clipping loss. The large single-mode beam size in a rotary disk laser will lead to high average power pulsed lasers operating at peak power levels unattainable in single-mode fibers with mode area constraint.

For the features mentioned above, it is anticipated that rotary disk laser will emerge as a very important class of high-brightness laser system in the future.

## Acknowledgments

The authors acknowledge useful discussions on rotary disk lasers with Dr. Harold Miller and Lt. Col. Roberta Ewart.